Ionics
https://doi.org/10.1007/s11581-026-07268-7

RESEARCH

Dual-functionalized sulfonated poly (arylene ether sulfone) membranes with sulfonamide crosslinks and octyl grafts for intermediate-temperature proton exchange fuel cells

Qana A. Alsulami[1] · Walid Mabrouk[2,4] · Sherif M. A. S. Keshk[3]

Received: 25 February 2026 / Revised: 2 June 2026 / Accepted: 5 June 2026

Abstract
Fluorine-free proton exchange membranes are increasingly required to replace perfluoro sulfonic acid (PFAS) materials in hydrogen fuel cells operating at low humidity and moderate temperatures. In this work, a one-step grafting–crosslinking strategy was used to fabricate a dual-functionalized sulfonated poly(ether sulfone) membrane (SPESOD) incorporating hydrophobic octylamine side chains and sulfonamide crosslinks via NH_2PES. This architecture enhances nanoscale phase separation, stabilizes ionic domains, and improves mechanical integrity at high sulfonation levels. The membrane exhibits an ion-exchange capacity of 1.1 meq/g, thermal stability above 250 °C, and a storage modulus exceeding 200 MPa. SPESOD achieves a proton conductivity of 0.14 S/cm at 120 °C and 100% RH, along with a proton transport number of $t^+ \geq 0.99$, indicating highly selective proton conduction. In single-cell fuel-cell testing, the membrane delivers a peak power density of 165 mW/cm^2 under the same conditions as Nafion® 117, demonstrating competitive performance. These results show that SPESOD provides a scalable, fluorine-free platform with a balanced combination of conductivity, mechanical robustness, and regulatory compliance for next-generation hydrogen fuel cells.

Keywords PFAS-free proton exchange membrane · Functionalization · Octylamine grafting · Sulfonamide crosslinking · Sulfonated polyether sulfone octyl di-sulfonamide (SPESOD) · Fuel cell performance · Sustainable energy materials

Introduction

Proton exchange membrane fuel cells (PEMFCs) are considered potential sustainable energy solutions for transportation, fixed power, and portable applications [1, 2]. Their efficiency and longevity are heavily reliant on the qualities of the proton exchange membrane (PEM), which must combine high proton conductivity, mechanical resilience, and chemical stability [3]. Nafion®, a type of perfluoro sulfonic acid (PFSA) membrane, is widely used due to its high conductivity in humid, low-temperature environments [4, 5]. However, its reliance on water for proton transport necessitates extensive humidification requirements and restricts system simplicity [6]. Intermediate-temperature PEMFC operation (100–140 °C) provides benefits such as improved electrode kinetics, increased CO tolerance, and easier thermal and water management [7]. However, at these temperatures, PFSA membranes experience severe dehydration and morphological collapse, resulting in significant conductivity losses and poor durability [8]. The environmental concerns and high cost of PFAS materials have fueled interest in PFAS-free alternatives [9]. Hydrocarbon-based PEMs are appealing possibilities due to their structural tunability, low cost, and promise for increased thermal stability [10]. SPES derivatives are known for their high ion-exchange capacity (IEC), oxidative resistance, and mechanical

✉ Walid Mabrouk
w.mabroukcerte@gmail.com

1 Chemistry Department, Faculty of Science, King Abdulaziz University, B.O. Box 80203, Jeddah 21589, Saudi Arabia

2 CERTE, Laboratory Water, Membrane and Environmental Biotechnology, BP 273, Borj Cedria, Soliman 8020, Tunisia

3 BECOME, Deep Tech & Nanoscience, 63 rue de Tolbiac, Paris 75013, France

4 Laboratory Water, Membranes and Environmental Biotechnology, Water Research and Technologies Center, Technologic Parc Borj Cedria, BP 273, Soliman 8020, Tunisia

Published online: 15 June 2026

strength [11]. Hydrocarbon membranes can experience swelling, limited phase separation, and impaired proton conductivity in low-humidity conditions [12]. Achieving a compromise between hydrophilicity, dimensional stability, and continuous proton-transport routes is a significant issue [13]. To address these limitations, dual-functionalization techniques combining hydrophilic and hydrophobic modifications have been investigated [14]. This study presents a novel SPES-based membrane (SPESOD) incorporating sulfonamide crosslinks and hydrophobic octyl grafts. The sulfonamide groups establish stable hydrogen-bond networks that support proton hopping even under low-hydration conditions, while the octyl chains promote nanoscale phase separation and suppress uncontrolled swelling [15]. This synergistic design aims to decouple proton transport from bulk hydration, permitting stable conductivity under intermediate temperatures and low humidity. Although there is increasing interest in these dual-modified hydrocarbon PEMs, little is known about their structure-property relationships and fuel-cell performance. In order to evaluate SPESOD's potential as a PFAS-free membrane for next-generation PEMFCs that operate beyond traditional humidity and temperature constraints, this study methodically investigates its physicochemical characteristics, proton-transport behavior, and single-cell performance in comparison to Nafion® 117.

Materials and methods

Chemicals, materials, and instruments

Chloro-sulfonated polyether sulfone (PES-SO_2Cl, Mw≈570 g/mol) and aminated polyether sulfone (PES-NH_2, Mw≈457 g/mol) were obtained from Eras Labo Society and used as the base polymer without further purification. Octylamine (OA, 99%) and N, N-dimethylacetamide (DMAc, anhydrous) were purchased from Sigma-Aldrich. Sodium hydroxide (NaOH) and sulfuric acid were obtained from Merck. All solvents were of analytical grade and used as received unless otherwise stated. Deionized water (resistivity≥18.2 MΩ.cm) was used throughout the membrane washing and conditioning steps. Nafion® 117 membranes were purchased from Sigma-Aldrich and used as commercial benchmarks for comparative analysis.

Synthesis of SPESOD membrane

The SPESOD membrane was synthesized via a one-step dual-functionalization strategy, as illustrated in Scheme 1.

Chloro-sulfonated polyether sulfone (SO_2Cl-PES, 5 g; 1.3 SO_2Cl groups per repeating unit) was dissolved in anhydrous DMAc (95 mL) to obtain a 5 wt% solution under a

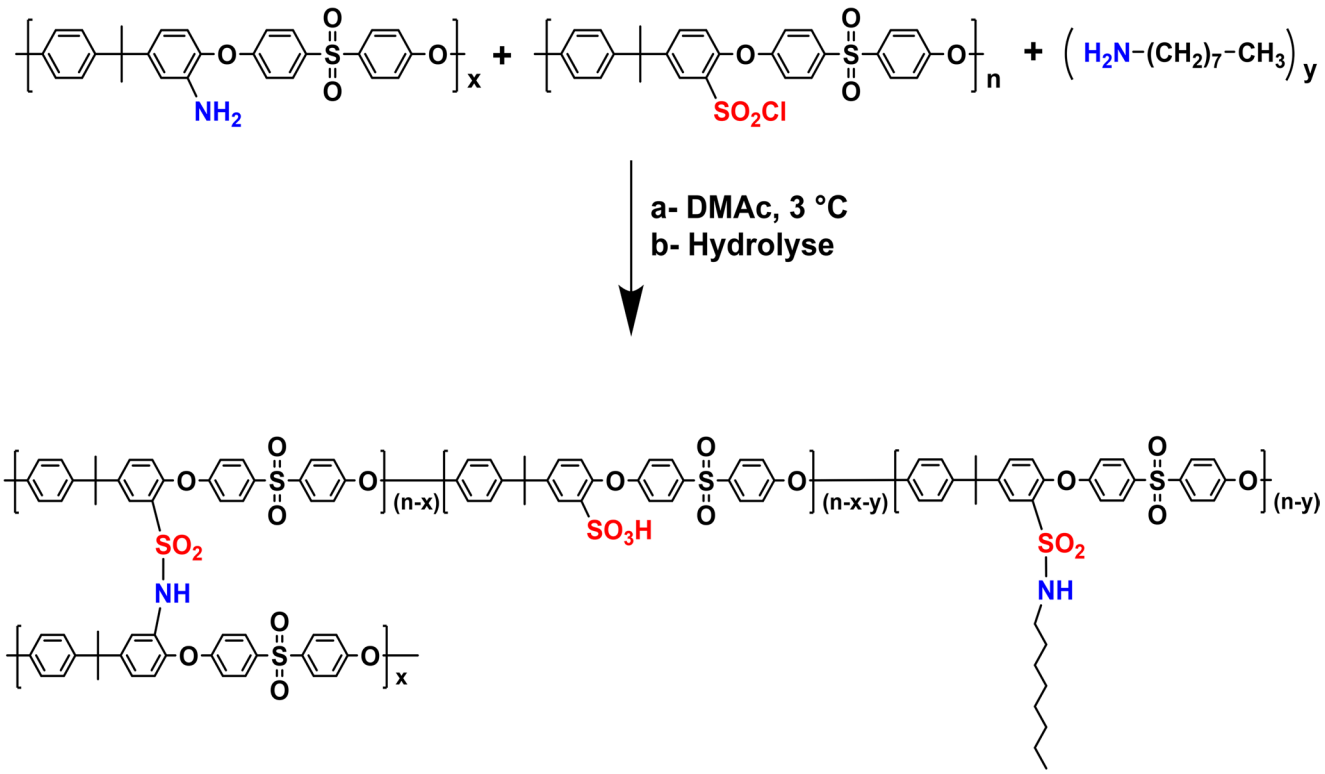

Scheme 1 Synthesis of SPESOD membrane via grafting and crosslinking of PES-SO_2Cl with octylamine and PES-NH_2

continuous nitrogen atmosphere. Octylamine (0.145 mL, 0.1 equiv.) and aminated PES (NH_2-PES, 0.4 g, 0.1 equiv.) were then added. The reaction was carried out in a three-neck round-bottom flask equipped with a magnetic stir bar and maintained under nitrogen to prevent moisture interference and to remove the HCl generated during substitution. To promote regulated nucleophilic substitution of the sulfonyl chloride groups, the mixture was stirring at 400 rpm under atmospheric pressure. The temperature was maintained at 4 °C for the first 15 min. using an ice-water bath. This one-step functionalization yielded the SPESOD architecture by grafting hydrophobic octyl-sulfonamide side chains and introducing covalent crosslinking with NH_2-PES through di-sulfonamide linkages. Grafting and crosslinking continued during the subsequent heat curing stage, hence no intermediate purification step was required. The reaction mixture (5 wt% polymer in DMAc) was cast directly onto a glass Petri dish and thermally cured in a ventilated oven at 50 °C (12 h), 70 °C (6 h), and 100 °C (6 h), allowing progressive solvent removal and completion of the functionalization reactions. After drying, the membranes were vacuum-dried to constant mass to ensure complete solvent removal. To eliminate remaining reactants and low-molecular-weight species, a homogeneous brown membrane (~100 µm thick) was peeled off, carefully rinsed with deionized water, and conditioned in 1 M H_2SO_4 for 24 h. The SPESOD membrane exhibited an ion-exchange capacity of 1.10 meq/g, equivalent to one proton for each repeating unit. Figure 1 shows a photograph of the SPESOD membrane in flat and somewhat bent forms.

The membrane has a uniform yellowish-brown hue, smooth and homogeneous surface morphology, and good flexibility without obvious cracking when bent, indicating successful membrane development and mechanical integrity. The membrane surface is smooth and defect-free, with no visible pores or fractures. This suggests that functional groups are evenly distributed throughout the polymer matrix. The constant thickness and dense, well-formed structure demonstrate effective control over the synthesis process, ensuring consistency of its physicochemical and mechanical properties.

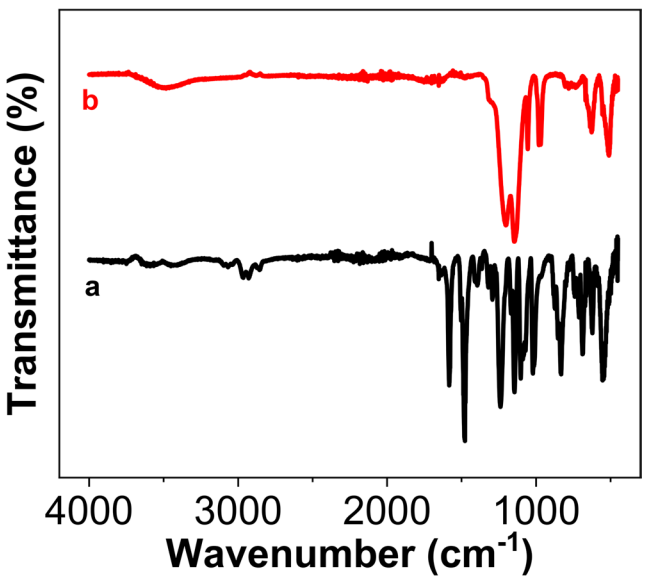

Fig. 1 A photograph of the SPESOD membrane

Membrane characterizations

A uniform conditioning protocol was used on the membranes before each characterization. After synthesis and acid treatment, the membranes were extensively rinsed with deionized water and dried under vacuum at 80 °C until constant mass was achieved to eliminate residual solvent and free water. The dried membranes were stored in a humidity-controlled desiccator (RH≈20–25%) to prevent uncontrolled moisture uptake. Membranes were re-equilibrated in distilled water for 12–48 h before testing for hydration-related characterizations such as water absorption, proton conductivity, and transport number. The unified pre-treatment resulted in consistent membrane conditioning across all physicochemical and electrochemical studies.

Physiochemistry characterizations

FT-IR data were collected using a Nicolet spectrophotometer (IR200 FT-IR) in transmission mode. The spectra of SPESOS and the different composite membranes were measured in the range 400 to 4000 cm^{-1}.

Thermogravimetric analysis (TGA) was performed using a Mettle TG analyzer. Samples weighing 2.5 mg were dried at 100 °C for 24 h to remove residual solvent. The TGA curves were recorded by varying the temperature from room temperature to 900 °C, at a heating rate of 10 °C/min with a flow of argon gas at a flow rate of 40 mL/min.

Differential scanning calorimetry (DSC) analyses were carried out using a TA Instruments device. Approximately 3 mg of the polymer sample was placed in the measurement cell, and thermograms were recorded over a temperature range of 20 to 300 °C at a heating rate of 5 °C/min. All measurements were performed under an argon flow of 40 mL/min.

Dynamic mechanical analysis (DMTA) was performed using a TA Instruments DMTA Q800 spectrometer operating in tensile mode. Membrane specimens were cut into 11 mm in length, 5 mm in width and 0.2 mm in thickness. Measurements were carried out under isochronal conditions at a frequency of 1 Hz, while the temperature increased

from room temperature to 300 °C at a rate of 3 °C/min. All experiments were conducted under a flow of dry argon at 50 mL/min.

All measurements (water uptake, contact angle, IEC, and conductivity) were performed on at least three independently prepared membrane samples. The published results represent the mean of these replicates, with standard deviations within ± 3–5% unless otherwise noted.

Electrochemistry characterizations

To determine the water uptake (WU), membrane samples were first dried in an oven at 80 °C until a constant mass was achieved. The dried membranes were then immersed individually in distilled water at room temperature for 48 h to ensure equilibrium hydration. The dry mass (W_{dry}) of each membrane was measured using an analytical microbalance with a precision of ± 0.01 mg. Before weighing, samples were dried in an oven at 80 °C until they reached a constant mass, defined as a fluctuation of less than 0.1% between two measurements taken 2 h apart. This method guarantees the total elimination of free water. The gravimetric method utilized here assesses total absorbed water (free + bound), which is common for hydrocarbon PEMs. Thus, the reported WU values indicate the combined water content relative to the dry polymer mass. After removal, any surface water was carefully blotted using hydrophilic filter paper. The hydrated membranes were weighed immediately, and WU was calculated from the difference between the wet and dry masses relative to the dry mass. From these values, the extent of water uptake was calculated [16], as the relative weight increase per gram of the dry sample using the following Eq. (1):

$$WU = \frac{W_{wet} - W_{dry}}{W_{dry}} * 100 \quad (1)$$

Where W_{wet} and W_{dry} are the weights of wet and dry membranes, respectively.

Contact angle (CA) measurements were carried out using a Theta Optical Tensiometer (Attention) on membrane specimens (1.5 cm × 1.5 cm). A 5 µL droplet of distilled water was carefully dispensed onto the membrane surface using a calibrated micro-syringe. The droplet profile was illuminated from behind and recorded with the instrument's integrated camera. The CA was determined using the Theta software by analyzing the droplet image at the point where no further change in shape was observed [17].

The cationic transport number was determined using Hittorf Cell. The cell consists of two symmetrical glass compartments separated by a membrane (4.15 cm^2), as described earlier [18, 19]. The proton transport number was calculated as described in the earlier work [12, 20]. The cell was filled with 1 M aqueous H_2SO_4.

The measurements were made for 188 min maintaining a current intensity of 100 mA. The amount of proton transfer is close to 10 mmol, considering the initial proton content in each compartment was 100 mmol.

The different proton membranes (area = 5 × 5 cm^2) were immersed separately in a sodium hydroxide solution (10^{-2} M) for 48 h [21, 22].

The ion exchange capacity was determined by an acid-base assay of the sodium hydroxide solution used to neutralize the membrane. The ion exchange capacity was determined by the relationship:

$$IEC = \frac{n^i_{N\alpha OH} - n^f_{N\alpha OH}}{W_{dry}} \quad (2)$$

where n^i_{NaOH} is the initial number of moles of sodium hydroxide solution (10^{-2} M, 200 mL), n^f_{NaOH} is the number of moles of sodium hydroxide after the exchange, and W_{dry} is the dry mass of the membrane.

Ionic conductivity of the membranes was evaluated by electrochemical impedance spectroscopy (EIS) using a Biologic VSP potentiostat. Measurements were performed at different temperatures under controlled relative humidity (RH) (0% and 100%). Disc-shaped membrane samples were mounted between two platinum-plated titanium electrodes. Proton conductivity was evaluated in a through-plane format with a two-probe impedance setup. The membrane was compressed between two blocking electrodes under constant pressure. For conductivity calculations, the active surface area was defined as the contact area between the membrane and the electrodes (S = 0.85 cm^2). The membrane resistance (R) was calculated using the high-frequency intercept of the Nyquist plot, minimizing electrode polarization effects [20].

This arrangement is commonly utilized for through-plane proton transport studies in hydrocarbon PEMs and enables reproducible comparison with Nafion® 117. Humidity was regulated in a sealed stainless-steel cell consisting of hot and cold compartments, with RH values calculated from the ratio of saturated vapor pressures at the respective temperatures. Nyquist plots were recorded over the frequency range 1000 kHz to 10 Hz with an oscillating voltage amplitude of 10 mV. The membrane resistance (R) was obtained from the high-frequency intercept on the real axis of the Nyquist plot [23, 24].

The membrane thickness (e) used in Eq. (3) was measured in the fully hydrated state immediately before each

conductivity experiment using a digital micrometer with ±1 µm precision. This procedure accounts for swelling (edema) and ensures an accurate determination of the effective proton-conduction path. The surface area (S) corresponds to the circular electrode–membrane contact area (1.33 cm^2), defined by the diameter of the platinum-plated titanium electrodes in the through-plane two-probe configuration. These parameters were applied consistently in all conductivity calculations. Ionic conductivity (σ, S/cm) was then calculated according to Eq. (3):

$$\sigma = \frac{e}{RxS} \tag{3}$$

where e and R denote the thickness and the electrical resistance, respectively, and S is the surface area of the membrane placed between the two electrodes.

Prior to fuel cell operation, the proton exchange membrane (SPESOD) was preconditioned by immersing it in distilled water for 12 h. A membrane Electrode Assembly (MEA) was subsequently prepared using commercial electrodes supplied by Paxitech. The membrane, with an active surface area of 64 cm^2, was placed between a hydrogen electrode and an oxygen electrode, each containing a platinum loading of 0.5 mg Pt/cm^2.

Before assembly, the catalytic layers of the electrodes were moistened with deionized water, and a thin coating of acidified silica gel was applied to the catalyst surface of each electrode to act as an interfacial binder. The use of acidified silica gel as an interfacial binder was chosen because it increases mechanical adhesion between the membrane and the catalytic layers while without affecting proton conduction or the MEA electrochemical performance. Silica-based binders are chemically inert under PEMFC operating conditions and do not engage in redox processes, hence performance variations between SPESOD and Nafion® 117 are exclusively due to membrane characteristics rather than interfacial artifacts. The thin acidic silica layer merely improves interfacial contact and reduces contact resistance, acting similarly to traditional ionomer binders but without introducing PFSA-derived effects that could skew results.

Fuel cell performance was assessed at room temperature under atmospheric pressure, with the partial pressures of hydrogen and oxygen maintained at 1 atm. Initial measurements were carried out using a Voltalab PGZ301 potentiostat/galvanostat, while higher current intensities (greater than 1 A) were supplied using an external current source. A high precision digital stem thermometer was securely positioned inside the PEMFC to enable continuous monitoring of the cell temperature during operation.

Results and discussion

Spectroscopic and thermal investigations were used to confirm the structural integrity of the synthetic SPESOD membrane. These characterizations sought to confirm the efficacy of the dual-functionalization strategy, octylamine grafting and sulfonamide crosslinking, as well as to identify the essential functional groups incorporated into the polymer backbone.

Fourier transform infrared spectroscopy

FTIR analysis was employed to identify the characteristic vibrational signatures of sulfonic acid, sulfonamide, and alkyl groups, providing direct confirmation of the SPESOD chemical structure. The FTIR spectrum of SPESOD (Fig. 2) clearly reflects the successful dual functionalization of the sulfonated poly(ether sulfone) backbone through covalent grafting of octylamine and crosslinking with aminated PES.

The main peak assignments are as follows: O–H stretching (~ 3400 cm^{-1}), aliphatic C–H stretching (2920–2850 cm^{-1}), N–H bending (~ 1650 cm^{-1}), aromatic C = C/C–C stretching (1580–1480 cm^{-1}), S = O asymmetric stretching (~ 1050 cm^{-1}), and SO_3H symmetric stretching (~ 1030–1010 cm^{-1}). These bands confirm the formation of sulfonamide and sulfonic acid groups and show no additional peaks attributable to impurities or undesired structures. In contrast, Nafion® 117 exhibits characteristic C–F and CF_2 vibrations near 1150 and 980 cm^{-1}, respectively, and its sulfonic acid bands are strongly hydration-dependent, reflecting a water-cluster-based conduction mechanism [25].

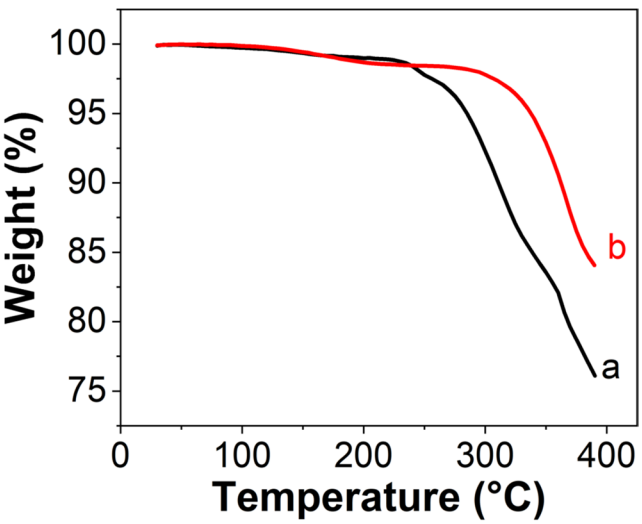

Fig. 2 FTIR spectrum **(a)** SPESOD **(b)** Nafion® 117

The absence of fluorinated bands in SPESOD, together with the presence of sulfonamide-specific and alkyl-chain vibrations, highlights its PFAS-free composition and validates its structurally distinct, environmentally compliant design.

Thermogravimetric analysis

Thermal stability constitutes a key parameter for proton exchange membranes (PEMs), especially in fuel cell applications where they operate under elevated temperatures and variable humidity conditions. The thermogravimetric analysis (TGA) was performed to evaluate the thermal degradation behavior of SPESOD and Nafion® 117 (H^+) membranes under a nitrogen atmosphere, in the temperature range from room temperature to 400 °C (Fig. 3).

Desorption of absorbed water causes a minor mass loss of ~ 2–3% at about 100 °C. Polymer-backbone thermal breakdown begins at about 250 °C after the initial water loss stage. SPESOD begins to show noticeable weight loss at approximately 250 °C, with a steep decline occurring between 300 °C and 370 °C. Nafion® 117 remains relatively stable up to approximately 300 °C, with a more gradual degradation onset and slower weight loss rate beyond that point. This contrast reflects fundamental differences in polymer architecture, bond strength, and functional group stability. The early onset of degradation in SPESOD is attributed to the presence of sulfonyl-octylamine grafts and chemical crosslinks. These functional groups, while enhancing proton conductivity and water retention, introduce thermally labile sites. Sulfonamide linkages begin to cleave around 250–300 °C, initiating mass loss [21].

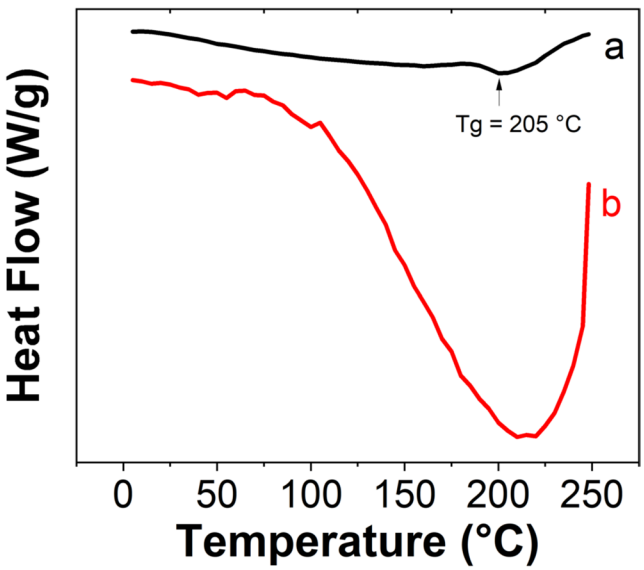

Fig. 3 TGA curves of **(a)** SPESOD **(b)** Nafion 117 (H^+)

Aliphatic octyl chains, introduced to improve flexibility and suppress excessive swelling, degrade more readily than aromatic backbones. Chemical crosslinking via aminated PES contributes to structural integrity but may also lower the decomposition threshold due to electrostatic interactions and localized chain mobility [12]. Despite this earlier degradation onset, SPESOD maintains structural integrity well above typical PEMFC operating temperatures (≤ 120 °C), indicating its potential for mid-temperature fuel cell applications, while its behavior under low-humidity operating conditions remains to be validated in-situ. Nafion® 117 exhibits superior thermal stability due to its perfluorinated backbone and highly crystalline domains. C–F bonds possess high bond dissociation energies (~ 485 kJ/mol), resisting thermal cleavage. The semi-crystalline morphology of Nafion® 117 contributes to delayed degradation, with significant mass loss only occurring beyond 350 °C. The gradual slope of curve B reflects the breakdown of sulfonic acid side chains followed by backbone scission. This thermal resilience makes Nafion® 117 suitable for high-temperature PEMFCs; however, its performance decreases under low-humidity conditions, and its PFAS content raises environmental concerns. Comparatively, SPESOD begins degrading earlier (~ 250 °C) and loses more mass by 400 °C (~ 25% residual), while Nafion® 117 retains slightly above 90% of its mass. SPESOD's aromatic backbone and functional grafts offer flexibility and tunability, while Nafion®'s perfluorinated structure ensures exceptional thermal endurance. SPESOD is PFAS-free and environmentally compliant, aligning with EU regulations, whereas Nafion® 117 faces increasing scrutiny due to its fluorinated content. While Nafion® 117 offers unmatched thermal stability, its drawbacks, PFAS content, high cost, and poor performance under dry conditions, limit its long-term viability. SPESOD, despite a lower degradation threshold, presents a compelling alternative. It remains thermally stable well above PEMFC operating temperatures, ensuring safe use in real-world systems. Its PFAS-free composition aligns with emerging environmental targets. The ability to tailor membrane properties via chemical grafting and crosslinking allows optimization for specific operating conditions, such as low humidity and moderate temperature. The TGA results confirm that SPESOD membranes are thermally robust enough for mid-temperature PEMFCs, particularly in decentralized hydrogen systems where environmental compliance and cost-effectiveness are prioritized. The trade-off between thermal stability and functional tunability is well-managed in SPESOD through intelligent design—balancing conductivity, flexibility, and degradation resistance. While Nafion® 117 remains the thermal benchmark, SPESOD offers a strategically engineered alternative that meets the evolving demands of sustainable fuel cell technologies.

Differential scanning calorimetry

DSC analysis provides complementary insight to the thermogravimetric analysis (TGA), focusing not on mass loss but on thermal transitions such as glass transition temperature (Tg), crystallization, and melting behavior. In this comparative DSC profile, the black curve represents SPESOD, while the red curve corresponds to Nafion® 117 (Fig. 4).

The heat flow was monitored over a temperature range of 0 °C to 300 °C, revealing distinct thermal behaviors that reflect the underlying polymer architecture and segmental mobility. The glass transition temperature (T_g) of SPESOD was found at approximately 205 °C, marking the transition from a rigid to an amorphous and soft state. This value is higher than that of commercial PES (187 °C) and SPESOS grafted only with 0.1 equivalent of octylamine (168 °C) or fully grafted with 100% octylamine (91 °C) [11], but lower than that of $ClNH_2$ crosslinked membrane with aminated PES (222 °C) [12]. The glass transition temperature (Tg) of PES- NH_2 was measured at 217 °C, while that of the Nafion® membrane is poorly resolved and ranges between 100 and 220 °C, depending on its hydration state [26]. This behavior consists of the presence of flexible aliphatic grafts and chemical crosslinking, which disrupt crystallinity and enhance segmental mobility without inducing distinct phase transitions.

The thermal stability of the heat flux profile supports the TGA results: SPESOD maintains its structural and energetic integrity well above operational temperatures, indicating potential for medium-temperature PEMFC applications, while its performance under low-humidity conditions still requires in situ validation. In contrast, Nafion® 117 has a broad endothermic feature between 100 and 220 °C, indicating water evaporation and thermal relaxation of the ionic domains. This thermal activity is associated with dehydration and reorganization of the ionic domains in Nafion® 117, particularly the collapse of hydrated sulfonic acid clusters, which makes it difficult to identify the glass transition temperature using DSC analysis. As the temperature increases, water molecules associated with the hydrophilic regions are expelled, leading to a temporary disruption of the polymer's microphase morphology. The sharp recovery in heat flow beyond 220 °C reflects the onset of backbone relaxation and possible reorganization of the semi-crystalline domains. This transition is not a melting point but rather a complex interaction between dehydration, ionic reconfiguration, and segmental motion. The previously established "exothermic decrease" is a broad endothermic feature, indicating the temperature range at which proton conductivity begins to decrease due to hydration loss. This behavior complements the TGA profile, where Nafion® retains its structure, but its functional performance is compromised under dry heat. The thermal-response instability observed in DSC highlights Nafion®'s dependence on water for maintaining ionic conductivity, which is a critical limitation in low-humidity or elevated-temperature environments. By comparison, SPESOD's stable DSC profile suggests that its proton conduction mechanism is less reliant on bound water and more dependent on fixed ionic sites and flexible chain dynamics. This decoupling of hydration from conductivity is a strategic advantage, enabling SPESOD to perform reliably under conditions where Nafion® falters. The absence of sharp thermal transitions also implies reduced thermal stress during operation, minimizing the risk of mechanical fatigue or phase separation. The DSC investigation supports SPESOD's thermally and energetically robust platform for proton exchange, complementing its structural integrity as established by TGA. While thermally resilient in mass retention, Nafion® exhibits energy instability at high temperatures, which impairs its functional performance. SPESOD is a next-generation membrane material designed for durability, environmental compliance, and operational versatility in fuel cell systems, according to its TGA and DSC profiles.

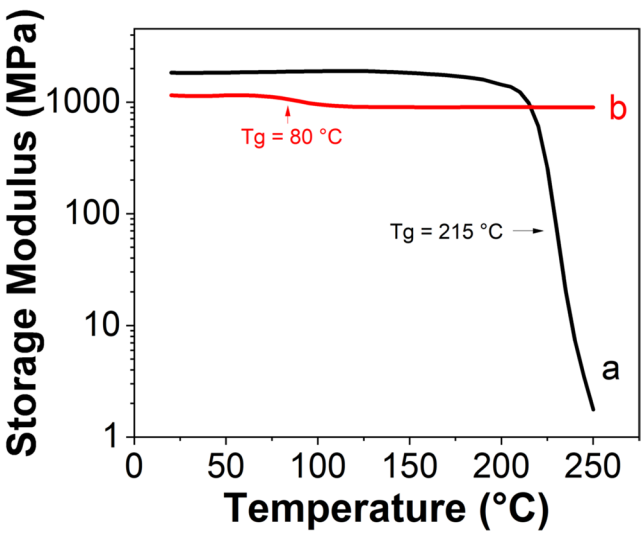

Fig. 4 DSC Curves of **a**. SPESOD **b**. Nafion 117 (H^+)

Dynamic mechanical thermal analysis

The DMTA curves illustrate the evolution of storage modulus with temperature for SPESOD and Nafion® 117, providing insight into their thermomechanical behavior and complementing the thermal transitions observed in DSC and TGA analyses (Fig. 5).

SPESOD exhibits a high initial storage modulus (~1800 MPa), indicative of a rigid polymer matrix at ambient conditions. However, a pronounced decline in modulus occurs around 200 °C, signaling the onset of

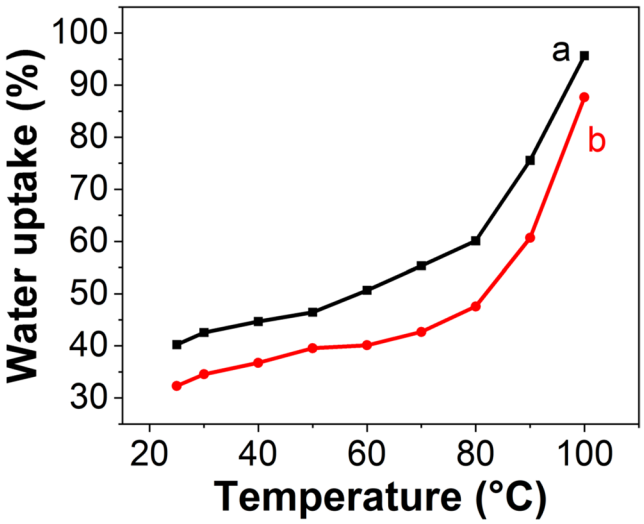

Fig. 5 DMTA Profiles of **a**. SPESOD **b**. Nafion 117 (H^+)

thermal softening or increased segmental mobility. This mechanical transition correlates with the exothermic event observed in the DSC thermogram, suggesting a glass transition or partial structural rearrangement. Simultaneously, TGA data confirms the onset of thermal degradation near this temperature range, reinforcing the interpretation that SPESOD begins to lose structural integrity beyond 200 °C. In comparison, Nafion® 117 exhibits an initial storage modulus (~1100 MPa), maintaining a relatively stable mechanical profile. A noticeable decrease occurs around 80 °C, corresponding to the transition from a rigid to a more flexible state.

This behavior aligns with its TGA profile, where thermal degradation typically begins above 280 °C. The sustained modulus underscores the robustness of Nafion®'s ionic architecture and its excellent thermal resilience, making it well-suited for high temperature applications requiring mechanical integrity. Combined analysis from DMTA, DSC and TGA indicate that although SPESOD demonstrates greater stiffness at lower temperatures, its thermomechanical stability is limited beyond 200 °C [27].

Static tensile measurements were conducted at room temperature using a universal testing machine (crosshead speed: 5 mm/min; gauge length: 10 mm) to confirm membrane flexibility. The SPESOD membrane has a Young's modulus of 180 MPa, a tensile strength of 12 MPa, and an elongation at break of around 22%. These values are within the range expected for flexible hydrocarbon PEMs with aliphatic grafts. The tensile behavior of sulfonated PES-based membranes is consistent with previously published profiles. Therefore, the whole stress-strain curve is not shown as the numerical values adequately characterize the mechanical response. Under comparable conditions, Nafion®117 typically has a Young's modulus of 150–200 MPa and an elongation at break of 150–300%. Nafion®, though less stiff initially, demonstrates exceptional thermal and mechanical endurance, highlighting the trade-offs between rigidity and high-temperature performance in membrane design.

Water uptake and ion exchange capacity

Water uptake and ion exchange capacity (IEC) are critical parameters that directly influence proton conductivity, dimensional stability, and electrochemical performance of proton exchange membranes (PEMs) (Fig. 6).

Figure 6 shows that the swelling ratio of both SPESOD and Nafion® 117 increases progressively with temperature, reflecting enhanced chain mobility and accelerated water diffusion at elevated temperatures. Across the entire temperature range, SPESOD exhibits consistently higher water uptake, increasing from ~ 40% at 25 °C to nearly 95% at 100 °C. The increase is gradual up to 70–80 °C, followed by a sharper rise at higher temperatures. In contrast, Nafion® 117 displays more moderate swelling, rising from ~ 32% at 25 °C to ~ 88% at 100 °C, with a noticeable increase only beyond 80 °C. This behavior indicates

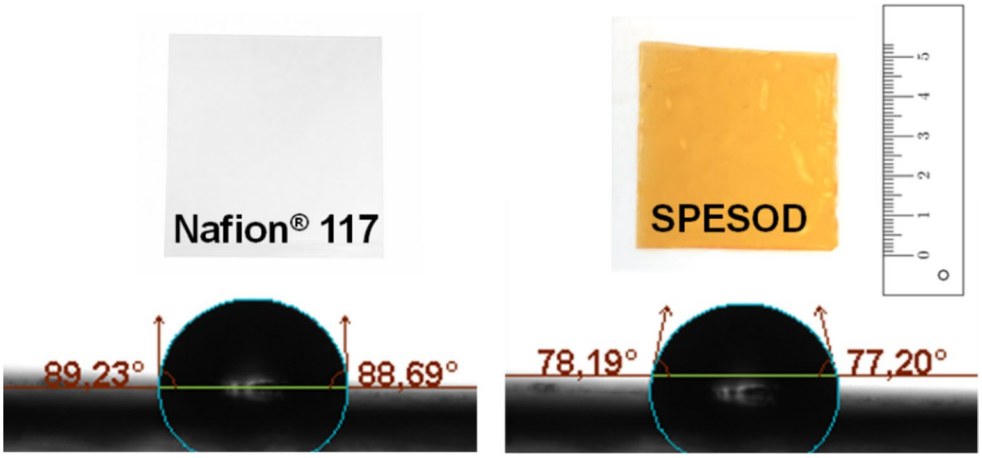

Fig. 6 Water uptake for **a**. SPESOD **b**. Nafion 117 (H^+)

that SPESOD possesses a stronger affinity for water, likely due to its combination of sulfonic acid groups, sulfonamide linkages, and microphase-separated domains that facilitate water retention. Importantly, unlike the unmodified SPES reference membrane (1.3 H^+ pmu), which dissolves near 60 °C, SPESOD maintains full structural integrity even in boiling water, demonstrating excellent thermal and hydrolytic stability [28, 29]. This robustness confirms the effectiveness of the dual-functionalization strategy in stabilizing the polymer network under harsh conditions. Although the IEC of SPESOD (1.10 meq/g) is close to that of Nafion® 117, this comparison is provided only as a contextual reference. The membrane's practical suitability for proton-conducting applications arises from the combined effect of its thermal stability, mechanical strength, controlled water uptake, and high proton conductivity.

At 25 °C, SPESOD exhibits a water uptake of 40.23% and an IEC of 1.10 meq/g, whereas Nafion® 117 shows 32.32% water uptake and a higher IEC of 1.25 meq/g (Table 1).

These values reflect resilience. The distinct hydration mechanisms and ionic site densities are inherent to each membrane's architecture. The higher water uptake in SPESOD is attributed to its sulfonyl-octylamine grafts and chemical crosslinking, which introduce hydrophilic domains and flexible aliphatic chains that facilitate water absorption. The octylamine groups, although individually hydrophobic, promote phase separation. Moreover, chemical crosslinking via aminated PES stabilizes the membrane morphology and when integrated into the sulfonated PES backbone, enables the formation of organized water channels, allowing controlled swelling without compromising mechanical integrity. SPESOD maintains a high modulus up to ~200 °C before softening, demonstrating that water uptake does not produce premature mechanical weakening. However, mechanical behavior under low-humidity operating conditions requires in-situ validation. In contrast, Nafion® relies on its perfluorinated backbone and pendant sulfonic acid groups to retain water. Its lower water uptake at 25 °C reflects the limited hydrophilic domain volume and the semi-crystalline nature of the polymer, which restricts water diffusion. However, the higher IEC of Nafion® (1.25 meq/g) indicates a greater density of ionizable sulfonic acid sites per gram of membrane, contributing to its superior proton conductivity under fully hydrated conditions. This ionic site density is a key reason why Nafion® remains the benchmark for PEMs, despite its limitations in dry or elevated-temperature environments. The balance between water uptake and IEC in SPESOD reveals a strategic trade-off. While its IEC is slightly lower than Nafion®, the enhanced water uptake compensates by improving proton mobility through better hydration of ionic pathways. This is particularly advantageous under low-humidity or intermediate-temperature conditions, where Nafion® suffers from dehydration-induced conductivity loss, as evidenced by the DSC dip near 200 °C.

Table 1 Water uptake and Ion Exchange Capacity of SPESOD and Nafion® at 25 °C

Membrane	Water uptake (%)	Ion Exchange Capacity (meq/g)
SPESOD	40.23	1.10
Nafion® 117	32.32	1.25

SPESOD's stable DSC profile and controlled swelling behavior suggest that its conductivity is less dependent on bound water and more reliant on fixed ionic networks and segmental flexibility. Furthermore, the TGA data supports the thermal viability of SPESOD, showing that despite its earlier degradation onset compared to Nafion®, it remains structurally intact well above operational temperatures. This ensures that the membrane can retain water and maintain ion exchange functionality without thermal collapse. The synergy between water uptake, IEC, and thermal/mechanical stability positions SPESOD as a robust candidate for mid-temperature PEMFCs, especially in decentralized or humidification-limited systems. In summary, SPESOD's higher water uptake and adequate IEC reflect a design optimized for hydration-driven conductivity and mechanical resilience. While Nafion® offers higher IEC, its lower water uptake and PFAS-based chemistry limit its adaptability in emerging clean energy frameworks. SPESOD's performance metrics, when viewed alongside TGA, DSC, and DMTA data, confirm its potential as a sustainable, scalable, and high-performing alternative for next-generation fuel cell membranes.

Contact angle

The contact angle measurements for SPESOD (77.20 ° −78.19 °) and Nafion® 117 (88.69 ° −89.23 °) show significant differences in surface wettability, reflecting the molecular design and hydration dynamics of each membrane (Fig. 7).

The larger contact angle of Nafion® indicates a more hydrophobic surface, which is consistent with its perfluorinated backbone and semi-crystalline structure, both of which limit water spreading and surface polarity.

SPESOD's decreased contact angle shows improved hydrophilicity, resulting from its dual-functionalized design that incorporates sulfonyl-octylamine grafts and chemical crosslinking with PES-NH_2. These alterations introduce flexible aliphatic chains and polar sulfonamide linkages, which aid in microphase separation and the development of hydrated domains. This structural arrangement not only enhances water uptake (40.23% vs. 32.32% for Nafion®) but also stabilizes the membrane shape during low-humidity

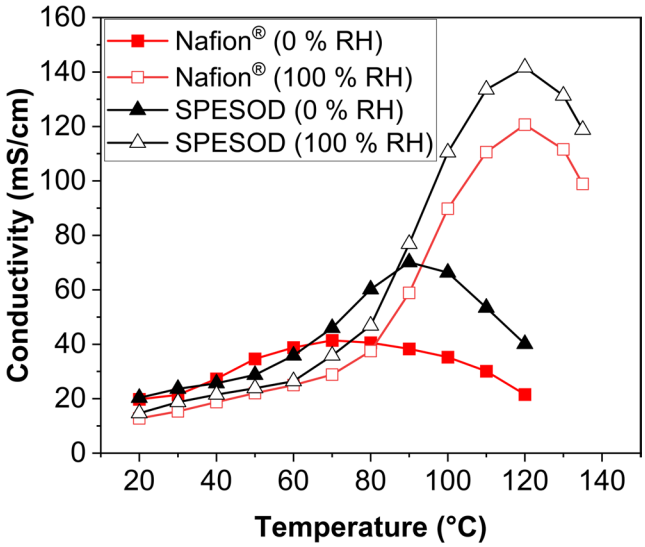

Fig. 7 Comparison between contact angle of Nafion® 117 and SPESOD membranes

conditions, as confirmed by DMTA and DSC investigations. SPESOD's reduced contact angle correlates with its capacity to sustain proton conductivity without external humidification, which is an important advantage for intermediate-temperature PEMFCs operating in decentralized or compact systems. Furthermore, the wettability profile promotes an efficient electrode-membrane interface, lowering interfacial resistance while improving electrochemical performance. Thus, the contact angle measurements support SPESOD's strategic balance of hydrophilic and hydrophobic domains, validating the design rationale and establishing it as a fluorine-free, regulatory-compliant alternative to Nafion® for next-generation fuel cell applications.

Proton transport number

Table 2 summarizes the transport number (t^+) values for SPESOD and Nafion® 117 membranes under different current intensities, measured using a Hittorf Cell. Under all tested conditions, both membranes exhibit remarkably high transport numbers (≥0.99), indicating predominant proton conduction and negligible contribution from counter-ions or other parasitic species. These results demonstrate that both the synthesized and commercial membranes possess excellent proton selectivity.

Table 2 Transport number (t^+) of SPESOD and Nafion® 117 membranes under varying current Intensities

Membrane	Surface (cm^2)	Current Intensity (mA)	Time (min)	$t^+_{Cathodic}$	t^+_{Anodic}
SPESOD	4.15	100	188	0.99	0.99
SPESOD	4.15	70	243	0.99	0.99
SPESOD	4.15	40	430	0.99	0.99
Nafion® 117	4.15	100	188	0.99	1.00
Nafion® 117	4.15	70	243	1.00	1.00
Nafion® 117	4.15	40	430	0.99	0.99

For SPESOD, the t^+ values remain stable at 0.99 for both cathodic and anodic directions across current intensities of 40, 70 and 100 mA.

This symmetry and consistency suggest a uniform proton transport mechanism, likely facilitated by the membrane's chemical crosslinking and sulfonyl-octylamine functional groups, which create well-defined, hydrated proton pathways. The absence of deviation with time or current intensity further supports the structural robustness and electrochemical stability of the SPESOD architecture. Nafion® 117, as expected, also demonstrates near-ideal transport numbers, with values of 0.99–1.00. Its performance is attributed to the well-established Grotthuss mechanism operating within its hydrated sulfonic acid clusters. However, the slight variation in t^+ between cathodic and anionic directions at higher current intensities may reflect localized dehydration or electro-osmotic drag effects, which are known to impact Nafion® under load [20]. The fact that SPESOD matches Nafion® in transport number while outperforming it in conductivity (Fig. 7), power density (Fig. 8b), and water uptake (Table 1; Fig. 5) highlights a key advantage: SPESOD achieves high proton selectivity without relying on perfluorinated chemistry or extensive hydration infrastructure. This makes it particularly suitable for intermediate-temperature PEMFCs, while its behavior in low-humidity environments, where maintaining a high t^+ is critical for minimizing fuel crossover and maximizing efficiency, still requires in-situ validation.

Proton conductivity

The proton conductivity profiles of Nafion® 117 and SPESOD membranes, measured at 0% and 100% relative humidity (RH) and presented in Fig. 8, reveal distinct temperature-dependent behaviors, reflecting their underlying transport mechanisms and hydration dynamics.

Under fully hydrated conditions (100% RH), both membranes exhibit increased proton conductivity with rising temperature. However, SPESOD consistently outperforms Nafion® 117 across the entire temperature range. This superior performance is attributed to the higher water uptake of SPESOD (40.23% vs. 32.32% for Nafion at 25 °C), which promotes the formation of continuous ionic channels and enhances proton mobility even at elevated temperatures. Nafion® 117 shows a maximum conductivity of 120 mS/cm at 120 °C, followed by a decline at higher temperatures, reflecting dehydration and disruption of its hydrogen-bonded water networks, which are crucial for the Grotthuss proton transfer mechanism [30]. SPESOD membrane, in

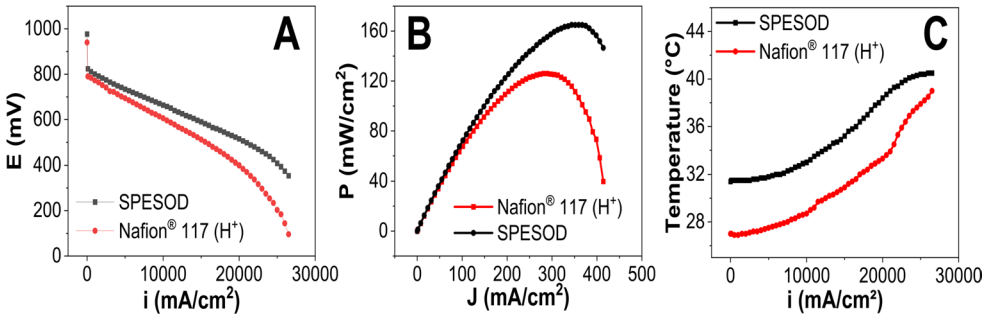

Fig. 8 Proton conductivity of Nafion® 117 and SPESOD membranes measured via EIS under 0% and 100% RH conditions

contrast, demonstrates a higher proton conductivity of approximately 140 mS/cm at 120 °C, indicating a transport mechanism dominated by hydronium ions (H_3O^+, $H_5O_2^+$) associated with retained water molecules [16]. The flexible sulfonic acid side chains and chemical crosslinking of SPESOD create microphase-separated domains that stabilize water and allow segmental mobility, thereby enhancing proton transport under thermal stress. Under anhydrous conditions (0% RH), conductivity decreases for both membranes.

However, SPESOD maintains superior ex-situ performance (70 mS/cm at 90 °C) compared to Nafion® 117 (40 mS/cm at 90 °C), highlighting intrinsic proton-conduction pathways that are less sensitive to hydration, while in-situ behavior under low-humidity conditions still requires validation. These trends are strongly correlated with water uptake, ion exchange capacity and thermomechanical behavior of the membranes. The high IEC and stable mechanical integrity of SPESOD up to 200 °C (confirmed by DMTA) preserve the conductive network, whereas Nafion® softens and dehydrates, compromising its performance. Overall, the architecture of SPESOD ensures robust proton conduction under varying humidity and temperature conditions, making it a promising candidate for intermediate-temperature PEMFCs and low-humidity applications where PFSA membranes such as Nafion® show limitations. Sulfonamide crosslinks and hydrophobic octyl grafts work together to establish a hydration-independent proton-transport network, which underpins SPESOD's superior low-humidity proton conductivity. Even when bulk water is limited, sulfonamide linkages (–SO_2–NH–) facilitate short-range Grotthuss-type proton hopping by forming directional hydrogen-bond bridges with adjacent sulfonic acid groups. Despite these benefits, numerous potential limits of SPESOD must be recognized for a meaningful PEMFC deployment. The presence of sulfonamide links and aliphatic grafts may diminish long-term oxidative stability under radical assault. Swelling control under variable humidity may still challenge hydrocarbon membranes, despite NH_2-PES crosslinking. Furthermore, the endurance of SPESOD at high current densities has not yet been assessed, and future research should focus on chemical stability, radical resistance, and extended MEA operation to completely establish its appropriateness for practical fuel cell conditions. These permanent hydrogen-bond donors and acceptors keep ionic domains from collapsing during dehydration and stabilize nearby proton-transfer sites. Concurrently, the flexible octyl chains provide nanoscale phase separation that concentrates acidic groups within percolated routes, while the NH_2–PES crosslinks limit excessive swelling and maintain the continuity of ionic nanochannels. This combination of structural stabilization and segmental mobility separates proton transport from water content, which explains why SPESOD retains conductivity while Nafion® undergoes dehydration-induced morphological collapse. Overall, the architecture of SPESOD ensures robust proton conduction under varying humidity and temperature conditions, making it a promising candidate for intermediate-temperature PEMFCs and low-humidity applications where PFSA membranes such as Nafion® show limitations. Sulfonamide crosslinks and hydrophobic octyl grafts work together to form a hydration-independent proton-transport network, which is responsible for SPESOD's better low-humidity proton conductivity.

Even in situations where bulk water is limited, sulfonamide linkages (–SO_2–NH–) can facilitate short-range Grotthuss-type proton hopping by forming directional hydrogen-bond bridges with adjacent sulfonic acid groups. These permanent hydrogen-bond donors and acceptors keep ionic domains from collapsing during dehydration and stabilize nearby proton-transfer sites. Concurrently, the flexible octyl chains provide nanoscale phase separation that concentrates acidic groups within percolated routes, while the NH_2–PES crosslinks limit excessive swelling and maintain the continuity of ionic nanochannels. This combination of structural stabilization and segmental mobility separates proton transport from water content, which explains why SPESOD retains conductivity while Nafion® undergoes dehydration-induced morphological collapse. Despite these benefits, numerous potential limits of SPESOD must be recognized for a meaningful PEMFC deployment. The presence of sulfonamide links and aliphatic grafts may diminish long-term oxidative stability under radical assault. Swelling control under variable humidity may still challenge hydrocarbon membranes, despite NH_2-PES crosslinking. Furthermore, the endurance of SPESOD at high current densities

has not yet been assessed, and future research should focus on chemical stability, radical resistance, and extended MEA operation to completely establish its suitability for practical fuel cell conditions.

Single-cell performance

The electrochemical performance of the synthesized SPESOD membrane was evaluated in a single-cell proton exchange membrane fuel cell (PEMFC) and benchmarked against commercial Nafion® 117 as shown in Fig. 9.

The polarization curves (Fig. 9a) reveal that SPESOD delivers a higher open-circuit voltage (~ 1 V, OCV) and maintains superior cell potential than the commercial membrane across the entire current density range. This enhancement reflects lower internal resistance and improved proton conductivity, consistent with the EIS results discussed earlier (Fig. 8). The steeper slope observed for Nafion® indicates more pronounced ohmic and activation losses, likely due to dehydration and limited proton mobility at elevated current loads. Figure 9b further confirms the superior performance of SPESOD, which achieves a peak power density of approximately 165 mW/cm^2 at 351 mA/cm^2, significantly higher than that of Nafion® (126 mW/cm^2 at 289 mA/cm²). This gain is attributed to the synergistic effect of SPESOD's high ion exchange capacity (IEC), enhanced water retention, and thermally stable morphology. The sulfonic acid-functionalized octylamine side chains and chemical crosslinking in SPESOD promote efficient proton transport and reduce mass transport limitations, even under high current draw. Moreover, the microphase-separated architecture facilitates water management, preventing flooding or drying, two common failure modes in PEMFCs. Figure 9c provides insight into the thermal behavior of the fuel cell during operation. SPESOD sustains higher operating temperatures across the current density range, indicating robust thermal stability and efficient heat dissipation. This is particularly advantageous for intermediate-temperature PEMFCs (80–150 °C), where Nafion® typically suffers from dehydration and mechanical softening [24]. The ability of SPESOD to maintain performance at elevated temperatures aligns with its DMTA and TGA profiles, which show mechanical integrity and minimal mass loss up to 200 °C. This thermal resilience ensures consistent proton conductivity and membrane durability under real-world operating conditions. Collectively, the data in Fig. 9 demonstrate that SPESOD not only surpasses Nafion® in electrochemical output but also offers operational advantages in terms of thermal stability and water management. These attributes position SPESOD as a promising candidate for next-generation PEMFCs, particularly in decentralized energy systems and harsh environments where conventional membranes underperform. The single-cell performance described here was obtained at near-ambient temperature and complete humidification, which isolates the intrinsic membrane contribution without introducing thermal or water-management aberrations.

The low power densities of both SPESOD and Nafion® 117 under these conditions are consistent with the known limitations of hydrocarbon membranes and PFSA materials at low temperatures. The MEA hardware and test station were not configured for controlled high-temperature, low-humidity operation, hence operating above 100 °C was excluded from this investigation. SPESOD's thermal stability (TGA), mechanical integrity (DMTA), and high temperature conductivity make it an excellent choice for intermediate-temperature PEMFCs. Future work will focus

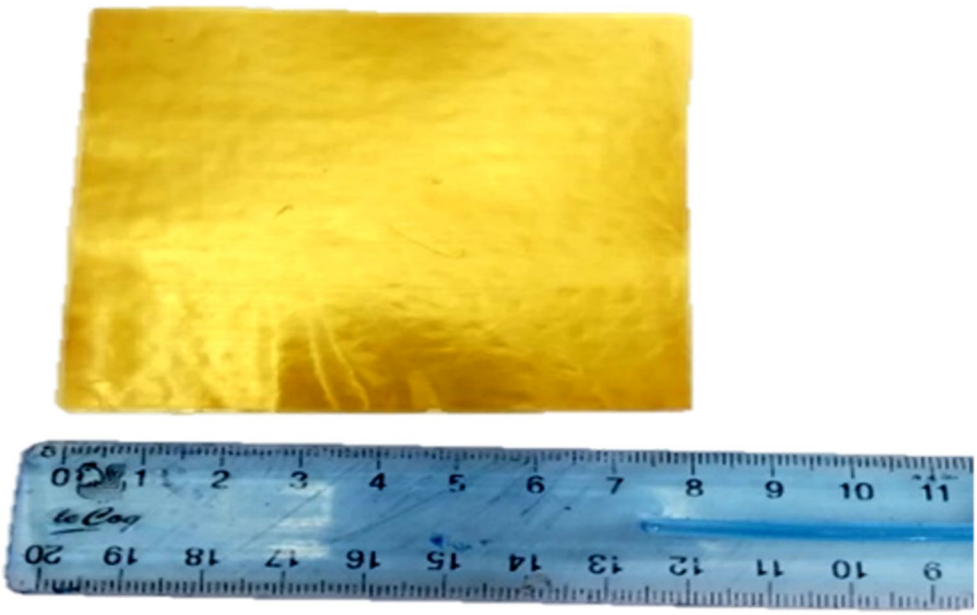

Fig. 9 Single-cell polarization and power-density curves of the SPESOD membrane measured at 25 °C under fully humidified H_2/O_2 (100% RH), atmospheric pressure, and gas flow rates of 100 mL/min (H_2) and 200 mL/min (O_2). **(A)** Polarization curves, **(B)** power-density curves, and **(C)** temperature behavior of the fuel cell during operation

on evaluating SPESOD under 100–140 °C and low-humidity conditions, including long-term durability and high-current-density operation, to fully validate its performance in realistic fuel-cell environments.

Benchmarking against reported PFAS-free polymer membranes

The SPESOD membrane was compared to other previously published PFAS-free polymer electrolyte membranes [30–38]. Benchmarking is conducted for sulfonated aromatic polymers, crosslinked hydrocarbon systems, nanocomposite-reinforced structures, and fluorine-free PEM technologies, focusing on key physicochemical and electrochemical indicators such as proton conductivity, ion-exchange capacity, thermal stability, and single cell performance. Table 3 presents relevant data from the literature and illustrates SPESOD's competitive performance. Its high-temperature proton conductivity, balanced IEC, robust thermal resistance, and high fuel-cell performance make it a promising PFAS-free PEM for long-term PEMFC operation.

Benchmarking results indicate that SPESOD ranks among the most competitive PFAS-free membranes reported in recent literature. It exhibits excellent proton conductivity at elevated temperatures, a well-balanced IEC, thermal stability above 250 °C, and strong single-cell performance. These attributes highlight the effectiveness of the dual-functionalization strategy. SPESOD surpasses other fluorine-free hydrocarbon PEMs in proton transport, mechanical integrity, and operational durability while remaining entirely PFAS-free. Overall, SPESOD represents a promising candidate for next-generation PEMFC systems that demand both sustainability and high performance.

Conclusions and futures perspectives

The work fabricated a fluorine-free proton exchange membrane by grafting and crosslinking sulfonamide linkages and hydrophobic octyl chains into a sulfonated poly (arylene ether sulfone) backbone. This dual-functional architecture relies on hydrogen bond networks to stabilize ionic domains and enhances nanoscale phase separation, allowing for continuous proton transport under dry ex-situ conditions. SPESOD membranes surpass traditional hydrocarbon membranes in terms of thermal stability, controlled swelling, and hydration-independent ex-situ proton conductivity. SPESOD's performance at near-ambient temperatures is unsatisfactory. However, physicochemical and electrochemical experiments reveal that it exhibits the structural and transport features required for moderate temperature performance. However, its performance in low-humidity fuel cells requires in-situ validation. These findings support the use of dual functionalization for the design of fluorine-free membranes that can mitigate PFSA dehydration limitations. Future study will investigate SPESOD's potential for next-generation sustainable fuel cells under 100–140 °C and low-humidity environments, including long-term durability and high-current density operation. The current study lacks dedicated oxidative stability measurements, which is a significant limitation. To fully determine the membrane's resistance to oxidative environments, systematic oxidative stability assessments such as Fenton's tests, radical degradation studies, and long-term durability evaluations are planned.

Table 3 Comparison of proton conductivity, IEC, thermal stability, and fuel cell performance of SPESOD with reported PFAS-free or hydrocarbon-based PEMs

Membrane	Conductivity (S/cm) (100% RH)	IEC (meq/g)	Temp (°C)	Power Density (mW/cm^2)	Ref.
SPESOD	0.14 at 120 °C	1.10	> 250	165	This work
Sulfonated PES–LDH/Sepiolite	0.085 at 80 °C	1.05	230	140	[30]
Hydrocarbon Pemion™ PEM	0.12 at 95 °C	1.20	260	180	[31]
Sulfonated aromatic polymer	0.10–0.13 at 80–120 °C	1.0 − 1.3	200 − 260	120 − 160	[32]
SPES with microphase separation	0.11 at 90 °C	1.15	240	150	[33]
Crosslinked SPES (DMAc-based)	0.095 at 80 °C	1.05	220	130	[34]
MOF-reinforced hydrocarbon PEM	0.12 at 120 °C	1.10	250	175	[35]
Silicate-reinforced sulfonated polymer	0.10 at 100 °C	1.08	240	150	[36]
Fluorine-free hydrocarbon PEM (Pemion™)	0.09 S/cm at 90 °C	1.9	250	110	[37]
Sulfonamide-functionalized polymer	0.11 at 110 °C	1.12	240	155	[38]

Author contributions Walid MABROUK: Validation, Methodology, Writing – review & editing. Qana A. Alsulami: Methodology, Data Curation, Funding Aquisition. Sherif M.A.S. Keshk: Conceptualization, Visualization, Writing – review & editing.

Funding This project was funded by the Deanship of Scientific Research (DSR) at King Abdulaziz University (KAU), Jeddah, under grant no (IPIP:705-247-2025). The authors, therefore, acknowledge with thanks DSR for technical and financial support.

Data availability Data will be made available on request.

Declarations

Competing interests The authors declare no competing interests.

References

1. Guo Z, Perez-Page M, Chen J, Ji Z, Holmes SM (2021) Recent advances in phosphoric acid–based membranes for high–temperature proton exchange membrane fuel cells. J Energy Chem 63:393–429
2. Kiani M, Zhao Y, Zhang R (2025) Proton exchange membrane fuel cells: recent developments and futures perspectives. Chem Commun 61(52):9392–9411
3. Maiti TK, Singh J, Dixit P, Majhi J, Bhushan S, Bandyopadhyay A, Chattopadhyay S (2022) Advances in perfluorosulfonic acid-based proton exchange membranes for fuel cell applications: A review. Chem Eng J Adv 12:100372
4. Qu E, Hao X, Xiao M, Han D, Huang S, Huang Z, Wang S, Meng Y (2022) Proton exchange membranes for high temperature proton exchange membrane fuel cells: challenges and perspectives. J Power Sources 533:231386, 231386
5. Haider R, Wen Y, Ma ZF, Wilkinson DP, Zhang L, Yuan X, Song S, Zhang J (2021) High temperature proton exchange membrane fuel cells: progress in advanced materials and key technologies. Chem Soc Rev 50:1138–1187
6. Ying J, Liu T, Wang Y, Guo M, Shen Q, Lin Y, Yu J, Yu Z (2024) Perspectives on membrane development for high temperature proton exchange membrane fuel cell. Energ Fuel 38:6613–6643
7. Raja Rafidah RS, Rashmi W, Khalid M, Wong WY, Priyanka J (2020) Recent progress in the development of aromatic polymer-based proton exchange membranes for fuel cell applications. Polymers 12:1061
8. Li X, Ye T, Meng X, He D, Li L, Song K, Jiang J, Sun C (2024) Advances in the Application of Sulfonated Poly(Ether Ether Ketone) (SPEEK) and its Organic Composite Membranes for Proton Exchange Membrane Fuel Cells (PEMFCs). Polymers 16(19):2840
9. Khatoo N, Alli N, Yang H, Jun (2024) Review of MOFs and their applications in the preparation of loose nanofiltration membranes for dye and salt fractionation. Desalin Water Treat 100092:100092
10. Wang M, Li L, Yan H, Yan X, Liu X, Li K, Li Y, You Y, Yang X, Song H, Wang P (2023) Poly(arylene ether)s-based polymeric membranes applied for water purification in harsh environment conditions : a mini-review. Polymers (Basel) 15(23):4527, 4527
11. Liu ML, Han X, He WW, Jiang FY, Ji F, Shen WW, Zhou T, Xu J, Ya–Qian L (2024) Sulfonated poly(aryl ether ketone sulfone modified by polyoxometalates LaW_{10} clusters for proton exchange membranes with high proton conduction performance. Tungsten 6:454–464
12. Seo DW, Lim YD, Lee SH, Jeong YG, Hong TW, Kim WG (2010) Preparation and characterization of sulfonated amine-poly(ether sulfone) s for proton exchange membrane fuel cell. Int J Hydrogen Energy 35:13088–13095
13. Mabrouk W, Charradi K, Kacem IB, Lafi R, Bellakhal N, Marzouki R, Keshk SMAS (2024) Significant augmentation of proton conductivity in low sulfonated polyether sulfone octyl sulfonamide membranes through the incorporation of hectorite clay. Mater Renew Sustain Energy 13:69–78
14. Zeng W, Guan B, Zhuang Z, Chen J, Zhu L, Ma Z, Hu X, Zhu C, Zhao S, Shu K, Dang H, Zhu T, Huang Z (2025) Comprehensive review on the advances and comparisons of proton exchange fuel cells (PEMFCs) and anion exchange membrane fuel cells (AFCs) : from fundamental principles to key component technologies. Int J Hydrogen Energy 102:222–246
15. Liao Y, Zhao S, Wang R, Zhang J, Li H, Liu B, Li Y, Zhang A, Tian T, Tang H (2025) Proton exchange membrane with dual-active-center surpasses the conventional temperature limitations of fuel cells. Adv Sci (Weinh) 12(10):2417259, 2417259
16. Jebri S, Mabrouk W, Elleuch R, Charradi K, Elhosiny Ali H, Ghorbel D, Keshk SMAS (2025) Dual proton transport in Schiff base-modified chitosan with AMPS for fuel cell applications. Mater Renew Sustain Energy 14:60
17. Dang DK, Zhou B (2024) Enhanced water management in PEMFC cathode using streamlined baffles. J Power Sources 623:235475
18. Agel E, Bouet J, Fauvarque JF (2001) Characterization and use of anionic membranes for alkaline fuel cells. J Power Sources 101:267–274
19. Barros KS, Marti-Calatayud MC, Scarazzato T, Bernardes AM, Espinosa DCR, Pérez-Herranz V (2021) Investigation of ion-exchange membranes by means of chronopotentiometry: a comprehensive review on this highly informative and multipurpose technique. Adv Colloid Interface Sci 293:102439, 102439
20. Mabrouk W, Charradi K, Lafi R, AlSalem HS, Maghraoui-Mehezi H, Keshk SMAS (2022) Augmentation in proton conductivity of sulfonated polyether sulfone octyl sulfonamide using sepiolite clay. J Mater Sci 57:15331–15339
21. Feng S, Shen K, Wang Y, Pang J, Jiang Z (2013) Concentrated sulfonated poly(ether sulfone)s as proton exchange membranes. J Power Sources 224:42–49
22. Kerres JA (2001) Development of ionomer membranes for fuel cells. J Membr Sci 185:3–27
23. Mabrouk W, Charradi K, Mellekh A, Hafiane A, Alsulami QA, Meherzi HM, Chtourou R, Keshk SMAS (2023) Enhanced Proton Conductivity of a Sulfonated Polyether Sulfone Octyl Sulfonamide Membrane via the Incorporation of Protonated Montmorillonite. J Electron Mater 52:2158–2167
24. Mabrouk W, Jebri S, Charradi K, Silimi B, Alzahrani AYA, Boubakri A, Ghodbane O, Raouafi N, Keshk SMAS (2023) Fabrication and Chracterization of graphene/sulfonated polyether sulfone octyl sulfonamide hybrid film with improved proton conductivity performance. J Electron Mater 27:991–999
25. Agarwal T, Prasad AK, Advani SG, Babu SK, Borup RL (2024) Infrared spectroscopy for understanding the structure of Nafion and its associated properties. J Mater Chem A 12:14229–14244
26. Jung HY, Kim JW (2012) Role of the glass transition temperature of Nafion 117 membrane in the preparation of the membrane electrode assembly in a direct methanol fuel cell (DMFC). Int J Hydrogen Energ 37:12580–12585
27. Rieger J (2001) The glass transition temperature tg of polymers – Comparision of the values from differential thermal analysis (DTA, DSC) and dynamic mechanical measurements (torsion pendulum). Polym Test 20:199–204
28. Mabrouk W, Lafi R, Fauvarque JF, Hafiane A, Sollogoub C (2020) New ion exchange membrane derived from sulfonated polyether sulfone for electrodialysis desalination of brackish water. Polym Advan Technol 32:304–314

29. Mabrouk W, Lafi R, Charradi K, Ogier L, Hafiane A, Fauvarque JF, Sollogoub C (2020) Synthesis and characterization of new proton exchange membrane deriving from sulfonated polyether sulfone using ionic crosslinking for electrodialysis applications. Polym Eng Sci 60:3149–3158
30. Hickner MA, Ghassemi H, Kim YS, Einsla BR, McGrath JE (2004) Alternative polymer systems for proton exchange membranes (PEMs). Chem Rev 104:4587–4611
31. Nguyen H, Klose A, Breitwieser M (2021) Hydrocarbon–based Pemion™ proton exchange membranes achieving state–of–the–art fuel cell performance. Sustain Energy Fuels 5:3687–3699
32. Lobato J (2021) Sulfonated aromatic polymer membranes for proton exchange membrane fuel cells: physicochemical and electrochemical performance evaluation. Polymers (Basel) 13:3064, 3064
33. Li X, Wang S, Zhang H, Lin C, Xie X, Hu C, Tian R (2021) Sulfonated poly (ether sulfone) membranes with controlled microphase separation for proton exchange membrane fuel cells. Int J Hydrog Energy 46:33978–33990
34. Yun G, Lee D, Bae I (2015) Dual–crosslinked sulfonated poly(ether ether ketone) membranes with isophthalic acids for enhanced proton exchange membrane fuel cells. J Power Sources 633:236450
35. Liang X, Zhang F, Feng W, Zou X, Zhao C, Na H, Liu C, Sun F, Zhu G (2013) From metal–organic framework (MOF) to MOF–polymer composite membrane: enhancement of low-humidity proton conductivity. Chem Sci 4:983–992
36. Mishra AK, Bose S, Kuila T, Kim NH, Lee JH (2012) Silicate-based polymer–nanocomposite membranes for polymer electrolyte membrane fuel cells. Prog Polym Sci 37:842–869
37. Nguyen H, Lombeck F, Schwarz C, Heizmann PA, Adamski M, Lee HF, Britton B, Holdcroft S, Vierrath S, Breitwieser M (2021) Hydrocarbon-based Pemion™ proton exchange membrane fuel cells with state-of-the-art performance. Sustain Energy Fuels 5:3687–3699
38. Zhang X, Li ZW, Chen XL, Chen DY, Zheng YY (2020) Side chain engineering of sulfonated poly (arylene ether)s for proton exchange membranes. Chin J Polym Sci 38:644–652